



# **Fuzzy Lead-Lag Controller Used In Control of Flexible AC Transmission System Devices**

C.Hareen Kumar<sup>1</sup>, P.Parvatheedeve<sup>2</sup>

PG Student (Power systems), Dept of EEE, Annamacharya Institute of Technology and Science, Tirupathi, A.P, India<sup>1</sup>

Assistant Professor, Dept of EEE, Annamacharya Institute of Technology And Science, Tirupathi, AP, India<sup>2</sup>

**ABSTRACT:** This paper proposes an evolutionary fuzzy lead-lag control approach for coordinated control of flexible AC transmission system (FACTS) contrivances in a multi-machine power system. The FACTS contrivances used are a thyristor-controlled series capacitor (TCSC) and a static var compensator (SVC), both of which are equipped with a fuzzy lead-lag controller to amend power system dynamic stability. The fuzzy lead-lag controller utilizes a fuzzy controller (FC) to adaptively determine the parameters of two lead-lag controllers at each control step according to the deviations of engenderer rotor speeds. This paper proposes an Advanced Perpetual Ant Colony Optimization (ACACO) algorithm to optimize all of the free parameters in the FC, which eschews the time-consuming task of parameter cull by human experts. The efficacy and efficiency of the proposed evolutionary fuzzy lead-lag controller for oscillation damping control is verified through control of a multi-machine power system and comparisons with other lead-lag controllers.

**KEYWORDS:** Ant colony optimization, flexible AC transmission system (FACTS), fuzzy control, static var compensator (SVC), swarm perspicacity, thyristor controlled series capacitor (TCSC).

## **I.INTRODUCTION**

POWER SYSTEM (PS) stability control is a consequential task in PS operation [1]. Several factors, such as external perturbances or internal mechanical torques, may facilely affect system stability. With the development of puissance Electronics, the structural control of electric power networks have recently magnetized more attention. In this context, flexible AC transmission system (FACTS) contrivances are becoming more popular. Due to their expeditious replication, these contrivances are acclimated to dynamically adjust the network configuration to enhance steady-state Performance as well as dynamic stability [2]–[5]. The availability of FACT contrivances, Such as thyristor-controlled series compensators (TCSCs), static var compensators (SVCs), and static synchronous series compensators (SSSCs), can provide variable turn and/or series emolument [3]. Thus, the control of these contrivances is very paramount [4]. TCSCs and SVCs have been widely studied in the technical literature and have been shown to significantly enhance system stability [6]–[8]. Therefore, this paper employs these two contrivances and proposes an incipient coordinated control scheme to enhance the dynamic replication of a multi-machine PS. Different FACTS contrivance control methods have been proposed for power oscillation damping and transient stability amelioration [9]. One popular damping control method utilizes a washout filter followed by the order lead-lag controller [10]–[14]. In general, the parameters of a lead lag controller are designed utilizing the pole-zero location method [11], [12], [14]. Modern PSs are astronomically immense-scale and in volute. This paper proposes a fuzzy lead-lag control scheme for the control and coordination of TCSC and SVC contrivances in a multi-machine PS. In this incipient control configuration, an FC is designed to adaptively adjust the parameters of lead-lag controllers at each control time step. Evolutionary fuzzy systems that design fuzzy systems population-predicated evolutionary computation techniques [17]–[20] have drawn attention in the past two decades. In contrast to genetic algorithms [17] and particle swarm optimization (PSO) [18], perpetual ACO, which finds solutions in a perpetual space, is a relatively incipient optimization approach [21]–[23]. In lieu of utilizing subsisting perpetual ACO algorithms, this paper proposes a novel ACO algorithm called Advanced Perpetual Ant Colony Optimization (ACACO). This paper is organized as follows. Section II describes the FACTS model. Section III introduces the fuzzy lead-lag control configuration. Section IV introduces the proposed ACACO.

# International Journal of Advanced Research in Electrical, Electronics and Instrumentation Engineering

(An ISO 3297: 2007 Certified Organization)

Vol. 4, Issue 3, March 2015

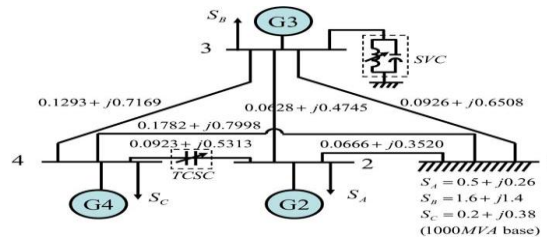


Fig.1. Multi-power system

Section V describes four examples of FACTS control quandaries. The performance of the proposed evolutionary fuzzy lead-lag control configuration is compared with that of different evolutionary control approaches. Determinately, Section VI presents the conclusion.

## II.SYSTEM MODEL

Fig. 1 shows a single-line diagram of the studied system consisting of three machines, three static loads, and an interconnecting network including mutually-coupled transmission lines radially connected to an illimitable bus [24]. The excitation system for the synchronous engenderer is the IEEE type 1 excitation system with constant prime mover mechanical torque. The system data are given in the Appendices. The damping for the three ascendant modes needs to be incremented, and the requisite for congruous stabilization equipment to damp out the multi-machine PS oscillations is evident. The TCSC is inserted into the transmission line between bus 2 and bus 4 to control the puissance flow. The block diagram for the TCSC model for typical transient and oscillatory stability studies is shown in Fig. 3 [16]. There are three inputs for sundry purposes: an auxiliary signal, , which could be the input from an external power flow controller, the reference, which is the initial operating point of the TCSC, and the diminutive-signal modulation input to provide stability. The configuration of a fine-tuned capacitor thyristor-controlled reactor (TCR) SVC is shown in Fig. 4. The nonlinear equipollent block diagram of the TCR part of the SVC is shown in Fig. 5. The equipollent admittance of the TCR can be obtained from

$$B_L(\alpha) = \left[ \frac{2\pi - 2\alpha + \sin 2\alpha}{\pi} \right] B_{L\text{MAX}} \quad (1)$$

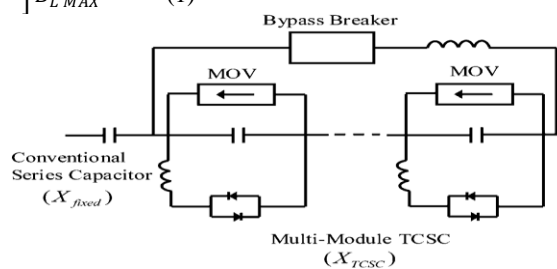


Fig. 2. Configuration of multimode TCSCs.

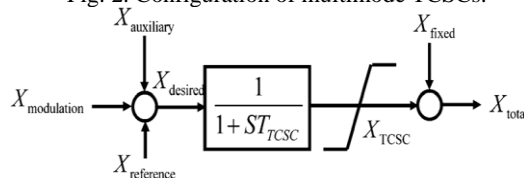


Fig. 3. Block diagram of TCSC model.

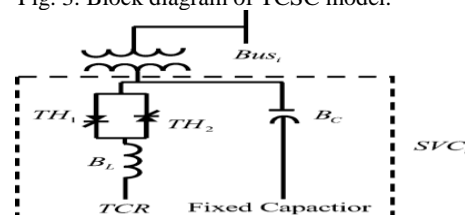


Fig. 4. Configuration of fine-tuned capacitor-TCR SVCs.

# International Journal of Advanced Research in Electrical, Electronics and Instrumentation Engineering

(An ISO 3297: 2007 Certified Organization)

Vol. 4, Issue 3, March 2015

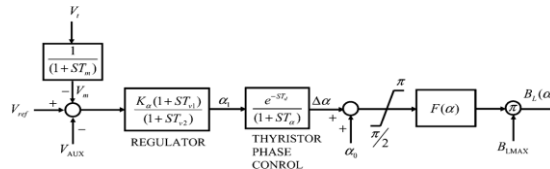


Fig.5. Block diagram of the SVC model

Where is the total admittance of the reactors relative to its MVA rating. The auxiliary controllers can give an adscitious control signal to the voltage regulator terminal. The Three-machine PS studied is simple but the proposed method is quite general and hence the application to more intricate cases can be facilely implemented by PS dynamic model reduction [25].

### III. EVOLUTIONARY FUZZY LEAD-LAG CONTROL CONFIGURATION

The cull of control inputs is very critical for wide area control. The most often used method to cull locations and stabilizing signals for PSSs and FACTS contrivances is controllability/ observability analysis predicated on a linearized time-invariant system model around a given operating condition [26], [27].

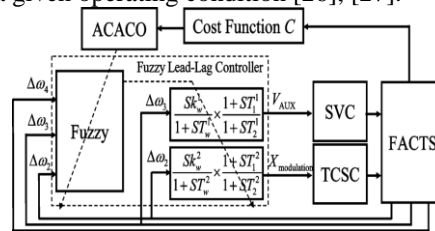


Fig.6. Evolutionary fuzzy lead-lag control configuration.

Since our proposed design method is applied directly to nonlinear system model, conventional engenderer rotor speed deviations [10], [16], [28] are culled as control inputs conservatively.

#### A. Lead-Lag Controller

This paper employs two lead-lag controllers to provide congruous control signals to the TCSC and the SVC.

$$\frac{V_{AUX}}{\Delta\omega_3} = \frac{SK_{\omega}^1}{1+ST_W^1} X \frac{1+ST_1^1}{1+ST_2^1} \quad (2)$$

$$\frac{X_{Modulation}}{\Delta\omega_2} = \frac{SK_{\omega}^2}{1+ST_W^2} X \frac{1+ST_1^2}{1+ST_2^2} \quad (3)$$

Where is speed deviation of the engenderer rotor to the reference speed .The lead-lag controllers send the modulation control signal ,to the TCSC, as shown in Fig. 3, and the auxiliary control signal, to the SVC, as shown in Fig. 5. The lead-lag controllers avail enhance the oscillation damping ability contributed by TCSC and SVC, thereby obtaining much higher calibers of stable power transfer.

#### B. Fuzzy Lead-Lag Controller

In the FC, there are three input variables, and which are speed deviations of the rotors in generatorsG2, G3, and G4, respectively. The outputs of the FC determine the values of the eight parameters in the two lead-lag controllers. The FC is composed of zero-order Takagi-Sugeno (TS)-type fuzzy IF-THEN rules with the following form:

Rule I: IF  $\Delta\omega_2(t)$  is  $A_1^i$  and  $\Delta\omega_3(t)$  is  $A_2^i$  AND  $\Delta\omega_4(t)$  is  $A_3^i$ , THEN  $T_1^i$  is  $a_1^i(t)$ ,  $T_2^i$  is  $a_2^i(t)$ ,

$T_W^i$  is  $a_3^i(t)$ ,  $K_W^i$  is  $a_4^i(t)$ ,  $T_1^2$  is  $a_5^i(t)$ ,  $T_2^2$  is  $a_6^i(t)$ ,  $T_W^2$  is  $a_7^i(t)$ ,  $K_W^2$  is  $a_8^i(t)$ ,  $i=1, \dots, R$  (4)

Where, is a crisp value, is the total number of rules, and each fuzzy set utilizes a Gaussian membership function, that is described by

$$\mu_j^i(\Delta\omega_k) = \text{Exp}\{(-\Delta\omega_k - m_j^i) / 2(b_j^i)^2\} \quad (5)$$

Represent the center and width of the fuzzy set, respectively. The firing vigor of the rule is computed by

$$\phi^i(x) = \mu_1^i(\Delta\omega_2) \cdot \mu_2^i(\Delta\omega_3) \cdot \mu_3^i(\Delta\omega_4) \quad (6)$$

The output of the FC described in (4) is denoted as, and is calculated by the following weighted average

Defuzzification formula:

$$Y_m = (\sum_{l=1}^R \phi^l \cdot a_m^l) / \sum_{l=1}^R \phi^l \quad (7)$$

The rotor speed deviations of all engenderers are utilized as controller inputs in order to evaluate the damping effect and determine the parameters of lead-lag controllers simultaneously. A modern PS has hundreds of engenderers. Then, the proposed approach can be utilized.

#### IV. ADVANCED PERPETUAL ANT COLONY OPTIMIZATION FOR FUZZY CONTROLLER OPTIMIZATION

##### A. Advanced Perpetual Ant Colony Optimization (ACACO)

The proposed ACACO works with a constant colony size of solutions (ants) at each learning iteration initially, the solutions are desultorily engendered. Each solution vector represents all of the parameters in an FC, i.e., a solution vector represents an FC. The solutions are sorted according to their performances from the best to the worst, and therefore, solution has rank. Fig. 7 shows a graphical representation of the ACACO algorithm in terms of nodes and path segments. The node values, in the throw represent values of the optimized variables in solution vector. Each path segment is associated with a pheromone level. ACACO consists of two phases. In the first phase ants start from the nest, move through nodes of variables and stop at the node of variable. The completion of the ant path constructs the ephemeral solution vector, denoted as where the values in the nodes visited constitute the ad interim solution components denoted as where the values in the nodes visited constitute the ad interim solution components. At each iteration, ACACO generates new solution (paths). An ant select a path segment with an exploration strategy. As in RCACO, elite and tournament selection techniques are used to implement exploration policies, respectively.

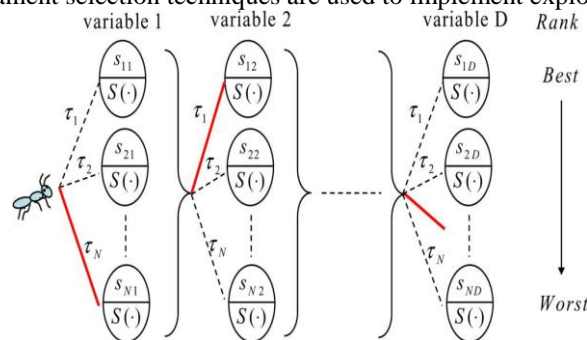


Fig. 7. Graphic representation of ACACO in terms of nodes and path segments, where an ant path is marked by a bold line.

In the contest collect, when an ant goes from variable to variable, three of the path segments are first culled desultorily and uniformly, regardless of the pheromone levels. Fig. 7 shows a path culled by the tournament cull method. In RCACO, the number of ephemeral solutions engendered from the two culls is identically tantamount at each iteration, i.e., As opposed to RCACO; ACACO utilizes an incipient distribution approach that dynamically. The number in the elite cull varies with the iteration number, and is given by

$$L(I_c) = Tx \left( \frac{I_c}{End\_ite} \right) \quad (8)$$

Where “End ite” is the total number of iterations. Equation (8) shows that the number of solutions engendered by the elite and tournament culls increase and decrement with iteration number, respectively. The second phase introduces incipient values to each node (solution component) via sampling of a Gaussian PDF and superseding the ad interim solution component, with the incipient sampled value. The component accommodates as the mean of Homogeneous to ACO in authentic space [22], the STD, of is computed as follows:

$$d_{ij} = \epsilon \cdot \sum_{t=1}^N s_{ij} - s_{ij} | \setminus (N-1) \quad (9)$$

This is calculated according to the distance from the culled node value to the other node values for the same variable. This paper utilizes an adaptive described by

$$\epsilon = f_{li} X \frac{I_c}{End\_ite} + f_{1f} \quad (10)$$



# International Journal of Advanced Research in Electrical, Electronics and Instrumentation Engineering

(An ISO 3297: 2007 Certified Organization)

Vol. 4, Issue 3, March 2015

The value of incrementations from to as learning evolves to evade premature convergence of the STD. Applying the Gaussian sampling operation to the ephemeral solution vector, gives an incipient solution vector, denoted as in ACACO, where

$$s_i^{new} = [s_i^{new} \dots \dots, s_{id}^{new}] = [S(g_{i1}(s_{i1})), \dots, S(g_{id}(s_{id}))], I=1, \dots, T. (11)$$

For each generation, a total of incipient solutions are engendered, and these solutions are deposited with the pristine solutions. These solutions are sorted from the best to the worst according their performance (i.e., according their cost values).

## B. FC Optimization through ACACO

In the ACACO-designed FC, the number of fuzzy rules is assigned in advance, and the number of fuzzy sets in each input variable is equipollent to the number of rules. All of the free parameters in the FC described in (4) are optimized. For the rule, there are two free parameters (and) for each of the three fuzzy sets in the antecedent part and eight free parameters in the consequent part. The performance of a solution vector is evaluated by a cost function that measures the control performance of the corresponding fuzzy lead-lag controller.

## V. SIMULATIONS

The following simulations were conducted on an Intel Core 2 quad-core-processor 2.83 GHz, running the Windows 7 operating system. The sampling interval in all examples was set to 0.001 s.

### A. Fuzzy Lead-Lag Control

Example 1 (Controller Design in Training Phase): This paper postulates that at 0.2 s, a sudden increment of 0.1 p.u. Mechanical torque occurs simultaneously at all three engenderers, G2, G3, and G4, and that this increment vanishes after 0.3 s. The control period is 0-9 s. Fig. 8 shows the dynamic replication of the speed deviations and the angles of the rotors in engenderers G2, G3, and G4 without utilizing the TCSC and SVC contrivances. The result shows that the system is proximately unstable without control. In applying ACACO to the evolutionary fuzzy lead-lag control quandary, the rule number, was set at 5, the colony size was set at 20 and was set at 10. The number of iterations was set at 1000. The FC should send control outputs to the PS within each sampling interval. In the simulations, it took only for the FC to send outputs for each incipient input data. The cost function, for performance evaluation was computed utilizing the root-mean-squared deviations of engenderer rotor speeds, and angles, 3 and 4, over 9000 time steps. The cost function is described as shown

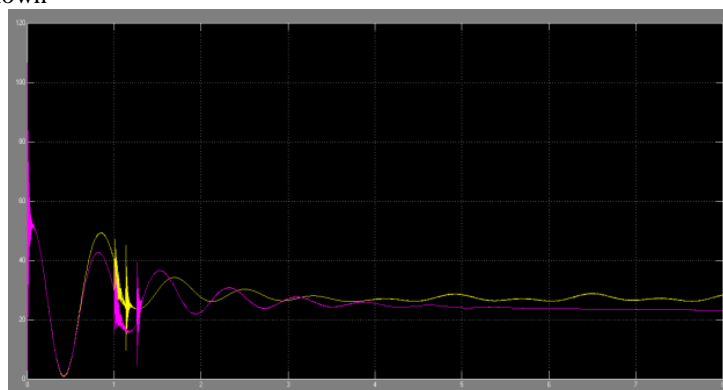


Fig. 8. Dynamic replication of rotor speed deviations and angles in G2, G3, and G4 utilizing fuzzy lead-lag controller, lead-lag controller and without control in Example 1, where a sudden increment of 0.1 p.u. mechanical torque occurs in G2, G3, and G4 at 0.2 s.

# International Journal of Advanced Research in Electrical, Electronics and Instrumentation Engineering

(An ISO 3297: 2007 Certified Organization)

Vol. 4, Issue 3, March 2015

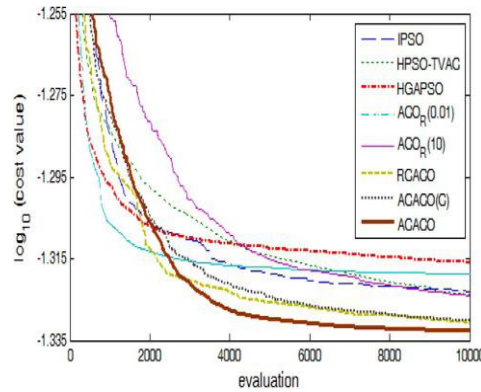


Fig. 9 Averaged best-so-far cost value at each evaluation for fuzzy lead-lag control through ACACO and several modified perpetual ACO and PSO algorithms.

As shown in Fig. 8, the angle deviation is about one thousand times the scale of the speed deviation. The speed deviation of engenderer G4 depends heavily on those of engenderers G2 and G3; therefore, the weighting was simply set to 1. Fig. 9 shows the best-so-far average value of at each evaluation. Table I shows the average (0.04650) and STD (0.00024) of the cost value, over the 30 runs. Fig. 8 shows the dynamic replication of the best

TABLE I

LEARNING PERFORMANCE OF ACACO AND SUNDRY PERPETUAL ACO ALGORITHMS FOR FUZZY LEAD-LAG CONTROL IN

Algorithms	ACO <sub>R</sub> ( $q = 0.01$ ) [22]	ACO <sub>R</sub> ( $q = 10$ ) [22]	RCACO [23]	ACACO(C)	ACACO
Average cost	0.04802	0.04743	0.04669	0.04675	0.04650
STD	0.001445	0.00067	0.00044	0.000460	0.00024
<i>t</i> -value	5.636	7.164	1.989	2.592	--

TABLE II

LEARNING PERFORMANCE OF ACACO AND MODIFIED PSO ALGORITHMS UTILIZING FUZZY LEAD LAG CONTROLLER IN EXAMPLE 1

Algorithms	HPSO-TVAC [18]	HGAPSO [19]	IPSO [20]	ACACO
Average cost	0.047457	0.048321	0.047514	0.046504
STD	0.000780	0.000998	0.000559	0.000244
<i>t</i> -value	6.387	9.687	9.070	--

The modified PSO algorithms utilized for comparison include a hierarchical PSO with a time-varying expedition coefficient (HPSO-TVAC) [18], a hybrid of the GA and PSO (HGAPSO) [19], and an ameliorated PSO algorithm (IPSO) [20]. Tables I and II show the performances of these perpetual ACO and PSO algorithms, respectively. Fig. 9 shows the best-so-far average values of at each evaluation of these perpetual ACO and PSO algorithms, respectively. Tables I and II show the *t*-values.



# International Journal of Advanced Research in Electrical, Electronics and Instrumentation Engineering

(An ISO 3297: 2007 Certified Organization)

Vol. 4, Issue 3, March 2015

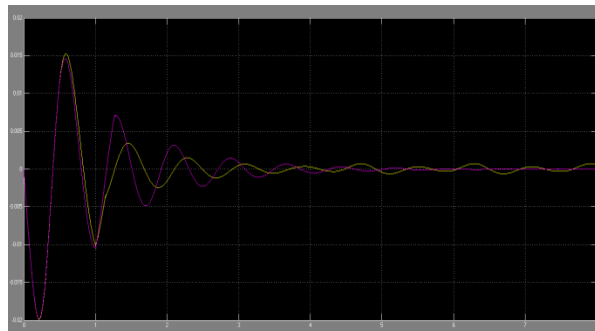


Fig.10. Dynamic replication of rotor speed deviations and angles in G2, G3, and G4 utilizing fuzzy lead-lag controller, lead-lag controller and without controlling Example 2.

TABLE III

PERFORMANCE OF FUZZY LEAD-LAG CONTROLLER AND LEAD-LAG CONTROLLER AT INCOMING SUDDEN INCREMENTS OF 0.01 P.U., 0.05P.U., AND 0.1 P.U. MECHANICAL TORQUE AT THE 2ND, 3RD, AND 4TH ENGENDERERS IN EXAMPLE 2

$\Sigma$	$ \Delta\omega_2 $	$ \Delta\omega_3 $	$ \Delta\omega_4 $	$ \Delta\delta_2 $	$ \Delta\delta_3 $	$ \Delta\delta_4 $
Lead-lag	0.001514	0.000398	0.002742	3.158593	0.749941	1.520297
Fuzzy lead-lag	0.001467	0.000315	0.001399	3.073404	0.653612	0.913832

The computational time for each run of the ACACO-predicated training approach took about 21 hours, which was about identically tantamount to those of the modified perpetual ACO and PSO algorithms utilized for comparison. The reason is that the time was mainly spent on computations of the PS outputs at each of the evaluations. The computational time of each population predicated learning algorithm is virtually negligible in comparison with the PS output computations.

TABLE IV

PERFORMANCE OF FUZZY LEAD-LAG CONTROLLER AND LEAD-LAG CONTROLLER AT UNKNOWN PERTURBATION AT THE 2ND, 3RD, AND 4TH TRANSMISSION LINES IN EXAMPLE 3

$\Sigma$	$ \Delta\omega_2 $	$ \Delta\omega_3 $	$ \Delta\omega_4 $	$ \Delta\delta_2 $	$ \Delta\delta_3 $	$ \Delta\delta_4 $
Lead-lag	0.000439	0.000134	0.000329	0.874215	0.215034	0.215149
Fuzzy lead-lag	0.000429	0.000078	0.000075	0.830994	0.136603	0.061266

Occur in one of the three engenderers, G2, G3, and G4. Three torque perturbations were arbitrarily engendered in the time interval [0, 5] s with magnitudes that were arbitrarily and uniformly engendered from the interval [0, 0.1] p.u. The duration of each perturbation lasted 0.1 s. The first increment of 0.085 p.u. mechanical torque occurred in G2 at 2.23 s, where it can be observed that the other two engenderers were additionally indirectly affected. At 3.33 s and 3.72 s, Table IV shows the DOLEFUL values of and in the control period [0, 12] s. Example 4 (Test Control with Faulted Lines): This example considers the contingency that a three-phase fault occurs on the transmission line between buses 1 and 2 in Fig. 1. The results show that controller prosperously damps the oscillations. Table V shows the WOEFUL vales of and (2, 3, and 4) in the control period [0, 7] s.

## B. Comparisons with Lead-Lag Controllers

This subsection supersedes the fuzzy lead-lag controller in Examples 1 to 4 with the lead-lag controllers in (2) and (3) for Comparative analysis. The parameter sets of the two lead-lag controllers were optimized utilizing ACACO with the cost function in (12) and the training condition utilized in the fuzzy lead-lag controller in Example 1.



# International Journal of Advanced Research in Electrical, Electronics and Instrumentation Engineering

(An ISO 3297: 2007 Certified Organization)

Vol. 4, Issue 3, March 2015

TABLE V  
PERFORMANCE OF FUZZY LEAD-LAG CONTROLLER AND LEAD-LAG CONTROLLER WHEN A FAULT OCCURS ON THE TRANSMISSION LINE BETWEEN BUSES 1 AND 2 IN EXAMPLE 4

$\Sigma$	$ \Delta\omega_2 $	$ \Delta\omega_3 $	$ \Delta\omega_4 $	$ \Delta\delta_2 $	$ \Delta\delta_3 $	$ \Delta\delta_4 $
Lead-lag	0.000196	0.000087	0.000871	0.467342	0.193137	0.465241
Fuzzy lead-lag	0.000156	0.000045	0.000578	0.366689	0.121561	0.304135

In comparison with the fuzzy lead-lag controller result shown in Table I, the  $\lambda$ -value was 31.151 and the null hypothesis was repudiated at the 1% significance level. In other words, the training performance of the fuzzy lead-lag controller is significantly better than the lead-lag controller. However, the results show that the fuzzy lead-lag controller damps the oscillations much more efficiently than the lead-lag controller. For quantitative analysis, Tables III–V shows the WOBEGONE values of  $\lambda$  and  $\sigma$  in Examples 2, 3, and 4, respectively, when utilizing the lead-lag controller. When utilizing the fuzzy lead-lag controller versus the lead-lag controller, which verifies the advantage of utilizing the proposed fuzzy lead-lag controller.

## VI. CONCLUSION

This paper proposes the simulation of two FACTS contrivances, an SVC and a TCSC, for the stabilization of a multi-machine PS. Simulation results in sundry conditions with different torque perturbations verify the Oscillation damping ability of the evolutionary fuzzy lead-lead control approach. In integration, comparison with the traditional lead-lag control approach shows the advantage of introducing the FC to adaptively determine the parameters in lead-lag controllers according to system status. The simulation results show that automatic optimization of the FC through the ACACO algorithm not only simplifies the design effort but additionally ameliorates the system dynamic replication. Comparisons with sundry modified perpetual ACO and PSO algorithms show the advantage of utilizing the ACACO algorithm in the PS stabilization quandary.

## REFERENCES

- [1] P. Kundur, J. Paserba, V. Ajjarapu, G. Andersson, A. Bose, C. Canizares, N. Hatziargyriou, D. Hill, A. Stankovic, C. Taylor, T. Cutsem, and V. Vittal, "Definition and classification of power system stability," *IEEE Trans. Power Syst.*, vol. 19, no. 2, pp. 1387–1401, May 2004.
- [2] J. J. Sanchez-Gasca, "Coordinated control of two FACTS devices for damping interarea oscillations," *IEEE Trans. Power Syst.*, vol. 13, no. 2, pp. 428–434, May 1997.
- [3] R. Mohan, Mathur and R. K. Varma, *Thyristor-Based FACTS Controller for Electrical Transmission System*. Piscataway, NJ: IEEE Press/Wiley Interscience, 2002.
- [4] K. Clark, B. Fradanesh, and R. Adapa, "Thyristor-controlled series compensation application study—Control interaction considerations," *IEEE Trans. Power Del.*, vol. 10, no. 2, pp. 1031–1037, Apr. 1995.
- [5] D. P. He, C. Y. Chung, and Y. Xue, "An eigenstructure-based performance index and its application to control design for damping interarea oscillations in power systems," *IEEE Trans. Power Syst.*, vol. 26, no. 4, pp. 2371–2380, Nov. 2011.
- [6] Y. C. Chang, R. F. Chang, T. Y. Hsiao, and C. N. Lu, "Transmission system locability enhancement study by ordinal optimization method," *IEEE Trans. Power Syst.*, vol. 26, no. 1, pp. 451–459, Feb. 2011.
- [7] X. Tan, N. Zhang, L. Tong, and Z. Wang, "Fuzzy control of thyristor-controlled series compensator in power system transients," *Fuzzy Sets Syst.*, vol. 110, pp. 429–436, 2000.
- [8] X. Lei, E. N. Lerch, and D. Povh, "Optimization and coordination of damping controls for improving system dynamic performance," *IEEE Trans. Power Syst.*, vol. 16, no. 3, pp. 473–480, Aug. 2001.
- [9] N. Mithulananthan, C. A. Canizares, J. Reeve, and G. J. Rogers, "Comparison of PSS, SVC, and STATCOM controllers for damping power system oscillations," *IEEE Trans. Power Syst.*, vol. 18, no. 2, pp. 786–792, May 2003.
- [10] M. E. Aboul-Ela, A. A. Sallam, J. D. McCalley, and A. A. Fouad, "Damping controller design for power system oscillations using global signals," *IEEE Trans. Power Syst.*, vol. 11, no. 2, pp. 767–773, May 1996.





ISSN (Print) : 2320 – 3765  
ISSN (Online): 2278 – 8875

# International Journal of Advanced Research in Electrical, Electronics and Instrumentation Engineering

*(An ISO 3297: 2007 Certified Organization)*

**Vol. 4, Issue 3, March 2015**

## BIOGRAPHY



C.HAREEN KUMAR was born in Tirupati, Chittoor (dis), AndhraPradesh, India, On November 11, 1991. He graduated from the KMM Institute of Technology and Science in 2012.He his Pursuing M.Tech specialization on POWER SYSTEMS in Annamacharya Institute of Technology and Science Affiliated to JNTU Anantapur.His research interests includes Power system stability, and energy storage systems.



P.PARVATHEE DEVI was born in January 3, 1988.She graduated from the Siddhartha Institute of Engineering and Technology in 2010. And Post graduated from Sri Venkateswara University SVU in 2013, Tirupati, Specialization on POWER SYSTEMS, Her research interests include Power system dynamics, stability, and energy storage systems.